X–ray spectroscopic study of effective plasma parameters in shock–ignition relevant plasmas

M.Šmíd[1,2], O.Renner[1], T.Pisarczyk[3], Z.Kalinowska[3]

[1] *Institute of Physics, Academy of Sciences CR, Prague, Czech Republic*

[2] *Czech Technical University in Prague, FNSPE, Prague, Czech Republic*

[3] *Institute of Plasma Physics and Laser Microfusion, Warsaw, Poland*

Detailed knowledge of macroscopic parameters of the near-surface plasma provides important information for optimizing the laser energy transfer in shock-ignition scenarios. In series of experiments performed at the Prague Asterix Laser System (PALS [1]), anomalous behaviour of the plasma parameters has been observed in dependence on the laser intensity [2]. Here we present precise x-ray spectroscopic data used to analyze environmental conditions in the plasma studied and provide theoretical model explaining experimental observations.

The effective temperature and density obtained by means of x-ray spectroscopy were measured on chlorine-doped plastic targets irradiated by laser with intensity varied over almost two orders of magnitude. The recorded spectra indicate that the temperature is only slightly increasing with the laser intensity, while the density increases approximately three times over the studied intensity range.

To understand these dependencies, a set of 2D hydrodynamic simulations have been performed and postprocessed using a collisional-radiative spectral code. The effective plasma parameters have been estimated from the resulting time– and spatially integrated synthetic spectra, and two diverse regimes were observed: At lower laser intensities ($< 5 \times 10^{14}$ Wcm^2), significant increase of the surface temperature and no change of the density with the increasing laser intensity was found. For the higher intensity range, corresponding to our experimental conditions, the temperature increase stopped while the effective density started to rise, in agreement with the experimental data.

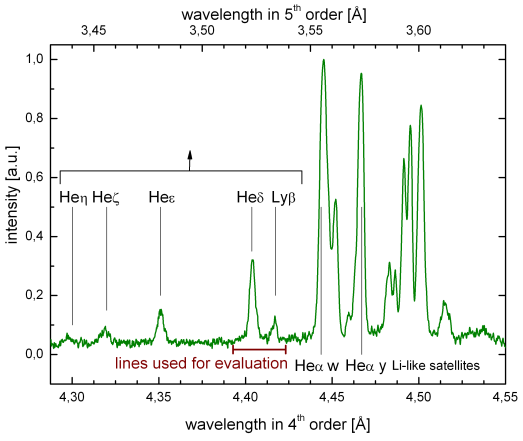

Figure 1: *Experimentally observed spectrum.*

Experiment

The experiment was performed with the PALS [1] main beam with wavelength $\lambda = 1315$ nm and pulse duration $\tau = 250$ ps. The focal spot diameter on the target surface was varied in the range $r_L = 50 \div 200$ μm and the energy between $50 \div 500$ J, altogether producing range of focused intensities $I = 5 \times 10^{14} \div 2 \times 10^{16}$ Wcm^2.

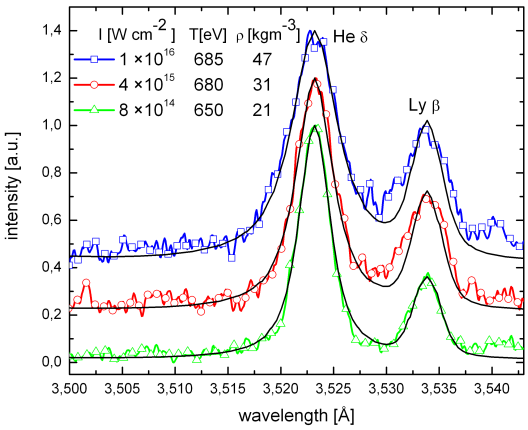

Figure 2: *Experimental spectra from three shots with various intensities (color) fitted with synthetic lineouts (black) and estimated parameters.*

The target was made of Cu substrate covered with a 25 μm thick layer of Cl–doped plastic (parylene-C). This material was chosen as the plastic mimics the outer layer of inertial confinement fusion pellet, and the Cl dopant was added because of diagnostic purposes. While most of present diagnostic complexes studied the shock wave velocity, plasma evolution, and parametric instabilities[4], this article focuses on the x–ray spectroscopic diagnostics only. This was realized by means of spectrometer employing spherically bent mica crystal ($2d = 19.84$ Å, $r = 150$ mm), the detection medium was an x–ray film. This spectrometer was setup to observe the H– and He–like Cl emission in 4^{th} and 5^{th} spectroscopical order. Both orders overlapped on the film, as seen in Fig. 1.

For the estimation of the effective plasma parameters, selected part of the experimental spectrum was compared to a set of synthetic spectra calculated by the PrismSpect code [3] for various temperatures and densities. The effective experimental parameters were then estimated as the parameters of the best fitting synthetic spectrum.

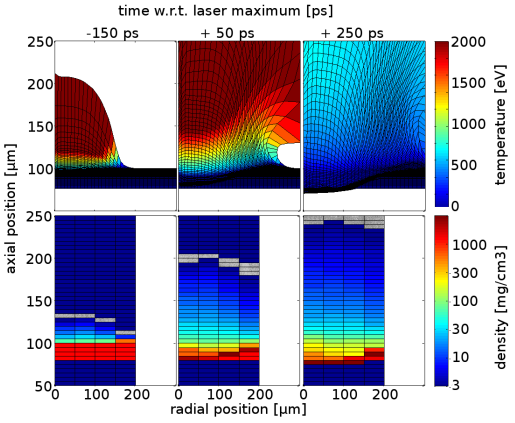

Figure 3: *Plasma evolution as calculated by the hydrodynamic simulation.*

For the evaluation, just the part of the spectra in the range $3.50 \div 3.55$ Å was used, as this region contains the He_δ and Ly_β lines. These lines are very suitable for parameter evaluation, because the the ratio of H– and He–like ions reflects the plasma temperature, while their width is sensitive to plasma density. Both lines have also relatively low optical thickness, thus the estimation is not significantly affected by the radiative transport. The result of fitting is shown in Fig. 2.

Modeling

The plasma evolution for various laser intensities was modeled by a 2D hydrodynamic code Multi2D [5], Fig. 3 presents the parameters from the hydrosimulation. The Lagrangian grid, shown in the top row with temperatures, had to be recalculated onto an Eulerian rectangular mesh (bottom row with densities), which is more suitable for spectral postprocessing. The gray areas in densities marks the laser critical density ($n_{e,\mathrm{crit.}} = 6.4 \times 10^{20}$ cm^{-3}, i.e. $\rho_{\mathrm{crit}} = 2$ mg cm^{-3}).

These hydrodynamic data were loaded into the Cretin collisional–radiative code[6], which calculates the population distribution and spectral emissivity for each cell and time of the data. Finally it performs the line–of–sight and time integration, creating synthetic spectra (Fig. 4) which can be directly compared to the experimental ones. With these spectra, the same procedure of evaluation of effective parameters was done as was done as in the case of experimental data.

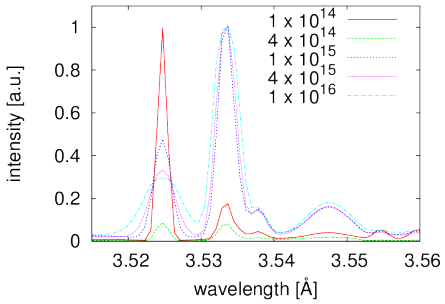

Figure 4: *Synthetic spectra. Each spectrum represents one postprocessed hydrosimulation, with given laser intensity [W cm^2].*

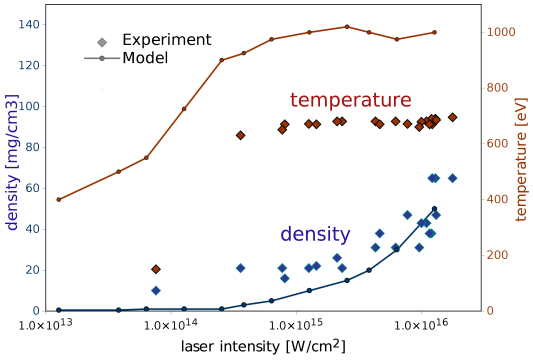

Figure 5: *Comparison of experimentally observed effective plasma parameters with the parameters obtained by postprocessing of simulations.*

Results and discussion

The results of both experiments and simulations are summarized in Fig. 5. For experimental data in the intensity range $5 \times 10^{14} \div 2 \times 10^{16}$ Wcm^2, the temperature is increasing very slowly from about 650 till 700 eV, however the density is growing exponentially from 20 to 60 mg cm^{-3}. The simulations reconstruct this behaviour qualitatively, however they predict much higher ($\approx$ 1000 eV) maximal temperatures.

To investigate this behaviour, the time and spatial profiles of relevant emission were studied in the output from spectral simulations. Fig. 6 reveals a spatial separation of production of both lines of interest: The He_δ line is emitted in the denser plasma close to the target surface, while the Ly_β is emitted dominantly further from the target. This separation, however, does not affect the measurement significantly. This figure also shows that the radiation is dominantly emitted during the time interval 0 ± 200 ps around the laser peak maximum.

Further comparison is shown in Fig. 7: 1D resolved on–axis plasma distribution during laser peak maximum ($t = 0$) is represented by blue (density) and violet (temperature) lines. Red and green lines show the He and Ly emission intensity from Cretin spectral postprocessing (similarly as in Fig. 6). The horizontal markers represent the effective parameters obtained from the experiment: it reveals that they reproduce the values from hydrosimulations at $z \approx 100$ μm.

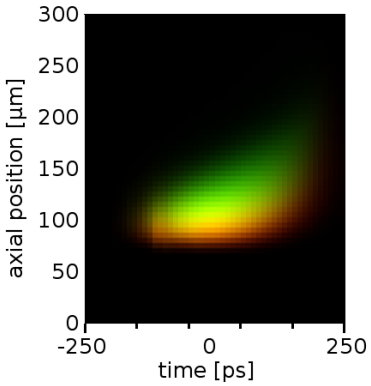

Figure 6: *Time and 1D (axially) resolved emission of He_δ (red) and Ly_β (green) spectral lines. Yellow color represents mixing of both color channels.*

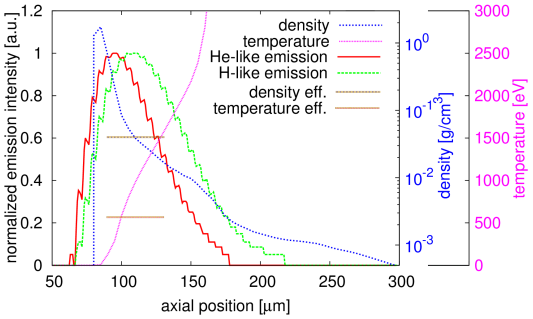

Figure 7: *Comparison of effective parameters to the hydrodynamic evolution.*

Finally, we can summarize these observations:

- The radiation is emitted in temporal interval ±200 ps around the laser peak maximum.
- The increasing density reflects the increase of pressure close to the target surface at higher intensities.
- Plasma pressure at the target surface can be estimated from observed parameters ranging between 150 GPa for low laser intensities till 700 GPa for the highest ones.
- A deeper understanding of the plasma behavior contributes to better interpretation of experimental results.

Acknowledgments

The research was done within the LASERLAB-EUROPE project No. pals001914 and was supported by the Czech Technical University grant SGS13/220/OHK4/3T/14 and the ASCR project M100101208.

References

[1] Jungwirth K et al 2001 Phys. Plasmas 2495 8.
[2] Guskov et.al. 2014 LPB 32 01.
[3] MacFarlane JJ et al 2007 HEDP 3 181-190.
[4] Batani D et al 2013 JPCS 399 012005.
[5] Ramis R et al 2009 Comput. Phys. Commun. 18 977-994.
[6] Scott HA 2001 JQSRT 71 689-701.